Proton-conducting Ordered Mesostructured Silica Monoliths

Liangming Xiong and Masayuki Nogami*
Department of Materials Science and Engineering, Nagoya Institute of Technology, Showa, Nagoya 466-8555

(Received May 8, 2006; CL-060530; E-mail: nogami@mse.nitech.ac.jp)

Ordered mesostructured silica monoliths (OMSMs) were prepared and after synthesis processed by a deep-UV irradiation to selectively oxidize their surfactants, and the UV-treated monolith exhibited a proton conductivity of 9.1×10^{-3} S cm^{-1}, much higher than that of the calcined monolith, via the first investigation into their AC impedance responses.

The structural features of mesoporous materials, such as narrow and controllable mesopore size (2–30 nm) and high specific surface area, make them be promising candidates in catalysis, separations, sensing, and optical and electronic applications.[1–3] Very recently, mesoporous materials have received an increasing attention and extensive investigation into their potential use as solid-state electrolytes for proton-exchange membrane fuel cells (PEMFCs), owing to their unique and favorable architectures. For example, Max Lu et al. reported sol–gel-derived zirconium phosphates with proton conductivities of about 10^{-8}–10^{-6} S cm^{-1};[4] Zhou et al. reported the synthesis of mesoporous nanocomposite with high proton conductivity up to 2×10^{-2} S cm^{-1}.[5] Our group reported pore-controlled mesoporous silica films with a proton conductivity in the range of 10^{-6} S cm^{-1} and ordered phosphosilicate glass electrolyte film with low area specific resistivity.[6,7] OMSMs with desired dimensions can be prepared via many methods[8–11] and may be an ideal candidate for a solid-state electrolyte. However, for OMSMs, a primary problem is the occurrence of macrocracks during the postsynthesis processing, including the selective or complete removal of their surfactants, which limits their further modification and application. Moreover, most of the current efforts have been focused on the uses of mesoporous powders in the form of pressed pellet and thin films as possible electrolyte alternatives for PEMFCs, but little was focused on mesostructured monoliths. Therefore, to develop a postsynthesis processing for OMSMs without macrocracks is necessary for such applications as solid-state electrolyte.

Herein, we present the preparation of large-size crack-free OMSMs using triblock nonionic copolymers, pluronic P123 ($EO_{20}PO_{70}EO_{20}$, MW 5800), as structure-directing agents and the selective removal of the surfactant employing a deep ultraviolet (UV) irradiation technique. An investigation is for the first time conducted into their proton conductivity.

The monolithic samples were synthesized in the following manner: pluronic P123 was added to an ethanolic HCl solution and kept being stirred to form homogeneous solution, followed with the addition of tetraethoxysilane (TEOS). After further stirring for 30 min, a transparent polymeric silica sol was formed with a final molar composition of CH_3CH_2OH:H_2O:HCl:P123:TEOS = 1:0.11:0.002:0.002:0.1. The silica sols were transferred into polystyrene vessels, and after aging at room temperature for about 20 days, silica gels were formed with a tunable thickness of 0.05–3 mm, and then transferred into a drying oven and kept under decreased pressure at below 50 °C. Finally, the resulting samples were placed under a deep-UV lamp with radiation at 187–254 nm, which is known to create ozone from atmospheric oxygen.[12] Au electrodes were coated on both surface sides of samples via evaporation for an AC impedance measurement (1E7–1 Hz). The conductivity was determined from the semicircle Nyquist plots, the thickness of the samples and the area of the gold electrode. For the purpose of comparison, the proton conductivity of a monolith calcined at 350 °C was examined in the same means.

Small-angle XRD (SAXRD, Philips, X'Pert-MPD) patterns (Figure 1A) of the UV-treated monolithic samples illustrate their ordered mesostructure. The diffraction peaks and their positions are very similar to those of mesoporous silica powder SBA-15,[13] indicating that the monolithic samples are of a 2D hexagonal mesostructure with space group *P6mm*.

To monitor the deep-UV oxidation process of surfactant, Fourrier transform infrared spectroscopy (FTIR) is available. Figure 1B shows the FTIR spectra (JASCO, FT/IR 460) of the as-prepared (a), UV-treated (b), and calcined (c) samples. As compared with the spectrum of the as-prepared sample, a new strong absorption signal appeared on the spectrum of the UV-treated sample at around 1728 cm^{-1}, attributed to carbonyl group (C=O) stretching vibration from C–C chain. This indicates some of the C–O groups were oxidized under the radiation with the UV lamp. However, the surfactant pluronic P123 of the UV-treated sample were not oxidized completely, because many of other signals, such as those at around 1457, 1380, 1345, and 1290 cm^{-1} which are due to CH_2 scissor bending, CH_3 bending, CH_2 wagging, and C–O stretching (or CH_2 twist), respectively, were still present on the spectrum. According to Parikh's work,[14] surfactants of MTFs could be fast removed fully by deep-UV exposure, the partial oxidation of the UV-treated sample selectively took place in the surface layer, since the surface layer preferentially absorbs UV energy and accordingly is oxidized by the ozone created via oxygen absorbing a deep-UV light,[14] and monolithic sample was much thicker than MTFs. Moreover, the absorbance at about 960 cm^{-1}, attributed to $Si^{\delta+}$–$O^{\delta-}$ stretching vibration of Si–OH groups[15] was detected and still very strong

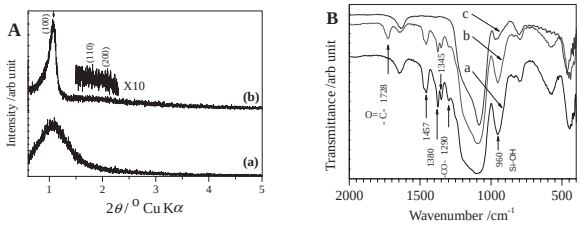

Figure 1. (A) Small-angle XRD patterns of UV-treated sample, a) before and b) after a treatment in a 100%-RH stream at 98 °C for 60 h; (B) FTIR spectra of the (a) as-prepared, (b) UV-treated, and (c) calcined samples.

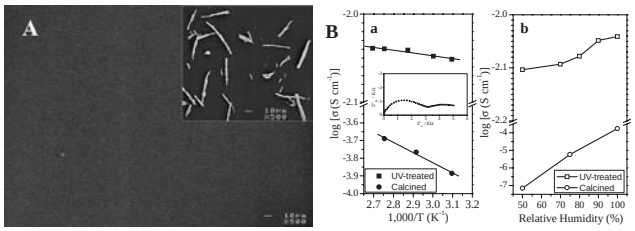

Figure 2. (A): SEM image of the UV-treated sample. Inset: SEM image of the worm-like particles of mesoporous silica SBA-15. (B): (a) Arrhenius plot for conductivities of the (■) UV-treated and (●) calcined samples under 100% RH condition; (b) Influence of water content on the conductivities of the (□) UV-treated and (○) calcined samples at 75 °C. Inset: a typical AC impedance response of the UV-treated sample.

on the spectrum of the UV-treated sample, but became much weaker on that of the calcinated sample. The mechanism of the oxidization is under further investigation.

Figure 2A gives a typical SEM image (JEOL, 6301) of the UV-treated monolithic sample, and in it no macrocrack was observed, much less the similar particle to the mesoporous powder (inset of Figure 2A) could be found. Thus, this deep-UV oxidation to selectively remove the surfactant may promise a mild postsynthesis processing for mesostructured monoliths.

The Si–OH bands generally play an important role on the proton conduction in porous silica glasses.[16] For the UV-treated sample, the above stronger absorbance of Si–OH bands to a certain extent implies a larger number of Si–OH groups it has, which are very useful for its proton conductivity. Its typical AC impedance response (Solatron 1260) was shown in inset of Figure 2B(a) and its conductivity was examined to be up to $9.1 \times 10^{-3}\,\mathrm{S\,cm^{-1}}$ at 98 °C under relative humidity (RH) 100%, as shown in Figure 2B(a). From the temperature and RH dependences of proton conductivity, as shown in Figure 2B, both temperature and RH increase the conductivity of both the UV-treated and calcined samples, and more significantly, the conductivity of the UV-treated sample is over an order of magnitude higher than that of the calcined sample under the same conditions. The calculated activation energies are 0.6 and $11.0\,\mathrm{kJ\,mol^{-1}}$ for the UV-treated and calcined samples, respectively. The activation energy may be related to the contents of SiOH bond and water inside sample, according to the previous work.[16] Generally, pore volume and specific surface area of porous proton-conducting membranes do strongly influence their conductivity via changing their water capability. Among our samples, the UV-treated sample must have lower pore volume and specific surface area in comparison with the calcined sample, since its surfactant was partly removed, whereas it exhibited much higher conductivity. This implies that its high conductivity was due to the crack-free framework wall, abundant Si–OH groups on wall surface, and even the unoxidized PEO units more than its pore volume and specific surface area. For proton conduction, crack-free framework wall serves as a continuous pathway; its surface, Si–OH groups act as a carrier via binding protons by weak hydrogen bonds and releasing them under an electrical field to transfer them from the initial site to a neighboring site, resulting in an electrical conductivity. Surfactant-containing mesostructured silica generally has three regions: siliceous matrix, hydrophobic core, and intervening interface,[17] thus the unoxidized hydrophilic PEO units in the intervening interface improved the water uptake ability of the intervening interface, benefiting the proton conduction in this region. On the other hand, unoxidized hydrophobic PPO units located in the core region and to some extent prevented protons diffusing through this region. Thus the interface conduction is the predominant mechanism. However, to improve proton diffusion in the surface layer can make it more possible for protons to be bound with the surface Si–OH groups via weak hydrogen bonds and further be released under an electrical field to be transferred. In this regard, the deep-UV radiation treatment benefited the high proton conductivity of the ordered mesoporous silica monolith.

Additionally, the unoxidized surfactant within the porechannels might support the ordered framework to prevent it from being fast disordered and collapsed. The SAXRD results (Figure 1A) confirmed the ordered mesostructures of the UV-treated monolith were kept after an 100%-RH stream treatment at 98 °C for 60 h, indicating its potential for PEMFC application for a certain period of time.

In summary, we demonstrated a template-assisted preparation and selective surfactant removal of large-sized, crack-free OMSMs. The UV-treated MSMs exhibited much higher proton conductivity than the calcined one. The levels of conductivity ($10^{-3}\,\mathrm{S\,cm^{-1}}$) achieved with the monoliths are not high enough for many applications. This work does, however, define a new direction in the search for a possible postsynthesis processing technique and solid-state electrolyte application of ordered mesostructured monoliths. There is much scope for further advancement of OMSM electrolytes.

This work was supported by the 21st Century COE Program in Nagoya Institute of Technology, Japan.

References

1 M. E. Davis, *Nature* **2002**, *417*, 813.
2 A. P. Wright, M. E. Davis, *Chem. Rev.* **2002**, *102*, 3589.
3 J.-L. Shi, Z.-L. Hua, L.-X. Zhang, *J. Mater. Chem.* **2004**, *14*, 795.
4 W. H. J. Hogarth, J. C. Diniz da Costa, J. Drennan, G. Q. (Max) Lu, *J. Mater. Chem.* **2005**, *15*, 754.
5 M. Yamada, D. Li, I. Honma, H. Zhou, *J. Am. Chem. Soc.* **2005**, *127*, 13092.
6 H. Li, M. Nogami, *Adv. Mater.* **2002**, *14*, 912.
7 H. Li, M. Nogami, *Chem. Commun.* **2004**, 236.
8 H. Yang, Q. Shi, B. Tian, S. Xie, F. Zhang, Y. Yan, B. Tu, D. Zhao, *Chem. Mater.* **2003**, *15*, 536.
9 S. A. El-Safty, T. Hanaoka, F. Mizukami, *Chem. Mater.* **2004**, *16*, 384.
10 H. Miyata, T. Suzuki, A. Fukuoka, T. Sawada, M. Watanabe, T. Noma, K. Takada, T. Mukaide, K. Kuroda, *Nat. Mater.* **2004**, *3*, 651.
11 Z. Zhang, B. Tian, X. Yan, S. Shen, X. Liu, D. Chen, G. Zhu, D. Zhao, S. Qiu, *Chem. Lett.* **2004**, *33*, 1132.
12 M. T. J. Keene, R. Denoyel, P. L. Llewellyn, *Chem. Commun.* **1998**, 2203.
13 D. Zhao, J. Feng, Q. Huo, N. Melosh, G. H. Fredrichson, B. F. Chmelka, G. D. Stucky, *Science* **1998**, *279*, 548.
14 A. M. Dattelbaum, M. L. Amweg, L. E. Ecke, C. K. Yee, A. P. Shreve, A. N. Parikh, *Nano Lett.* **2003**, *3*, 719.
15 M. S. Morsey, J. D. Bryan, S. Schwarz, G. D. Stucky, *Chem. Mater.* **2000**, *12*, 3435.
16 M. Nogami, R. Nagao, C. Wong, *J. Phys. Chem. B* **1998**, *102*, 5772.
17 L. Xiong, J. Shi, J. Gu, W. Shen, X. Dong, H. Chen, L. Zhang, J. Gao, M. Ruan, *Small* **2005**, *1*, 1044.

Published on the web (Advance View) August 5, 2006; doi:10.1246/cl.2006.972